Journal of Structural Geology 30 (2008) 1272–1287

Contents lists available at ScienceDirect

Journal of Structural Geology

journal homepage: www.elsevier.com/locate/jsg

From Adria- to Africa-driven orogenesis: Evidence from porphyroblasts in the Betic Cordillera, Spain

Domingo Aerden [a,*], Mohammad Sayab [b]

[a] Departamento de Geodinamica, Universidad de Granada, C/ Fuentenueva s/n, 18002 Granada, Spain
[b] National Centre of Excellence in Geology, University of Peshawar, Peshawar 25120, Pakistan

ARTICLE INFO

Article history:
Received 14 September 2007
Received in revised form 9 June 2008
Accepted 17 June 2008
Available online 9 July 2008

Keywords:
Betic Cordillera
Porphyroblast
Inclusion trails
Alpine tectonics
Mediterranean

ABSTRACT

In order to unravel the kinematic evolution of the Betic–Rif orogen, we investigated the geometry of porphyroblast inclusion trails in the Nevado-Filabride Complex, a high-pressure unit situated at the base of the Betic nappe stack. A large number of quantitative orientation data for these microstructures, and their mutual overprinting relationships, reveal two age groups of inclusion trails in the study area with distinctive geographic trends. Coupled to a comprehensive compilation of field data in the study area, these microstructures are shown to coherently witness the development of early NE–SW trending structures and fabrics, followed by younger NW–SE trending ones, whereby the former experienced clockwise reorientations. A major change in the direction of bulk crustal shortening from NW–SE to NE–SW is inferred from these data, and tentatively linked to the plate-tectonic history of the Mediterranean region. Paleomagnetic data indicate that, prior to about 35 Ma, NW–SE convergence between Adria, Eurasia and Iberia produced orogenesis along a belt bordering "Greater Iberia" (including Sardinian and Corsica) and probably continuous in the Alps (Briançonnais domain). The roughly NE–SW trend of this precursor appears to be preserved within porphyroblasts that grew during this period, presumably due to the partitioning of deformation around them. Africa–Iberia relative motion had been mainly transcurrent until 35 Ma (Azores transform), but then rapidly changed to head-on NNE–SSW convergence. This gave rise to a second set of NW–SE trending structures, which accompanied deformation of the precursor orogen into several oroclines (Western Alps, Gibraltar and Calabria Arcs). Orogenic collapse and crustal extension initiated shortly after this transition in tectonic regime suggesting a causal relationship. We propose that the waning of compressive stresses transmitted by Adria and their substitution by a near-perpendicular maximum stress direction resulting from Africa–Eurasia convergence could have enhanced the sinking of a thick lithospheric root or roll-back of a subducted slab, which in turn would have provoked crustal extension and basin formation.

1. Introduction

Despite almost a century of intensive geological research in the Betic–Rif orogen, the kinematic evolution of this remarkably curved mountain belt continues to raise fundamental questions. Highly variable tectonic transport directions have been deduced from stretching lineations and shear-sense indicators, whose spatial and temporal relationships have not been resolved in detail (cf. Martínez-Martínez and Azañon, 1997; Vissers et al., 1995). Structural overprinting relationships, although sometimes rationalized in terms of progressive deformation (Jabaloy et al., 1993; Augier et al., 2005a), appear to witness a superposition of different kinematic regimes of uncertain significance (Vissers, 1981; De Jong, 1993a, b). The nature (e.g. contractional versus extensional) or even existence of major tectonic contacts and structures also continues to be debated (e.g. Orozco et al., 1998; González-Lodeiro et al., 2004), as counts for the age of high-pressure metamorphism (e.g. Puga et al., 2004a; Augier et al., 2005b; Platt et al., 2006). In view of all this uncertainty, it is not surprising that different plate-tectonic models are considered envisaging oceanic or continental subduction, different subduction directions and different mantle processes (see review by Michard et al., 2002).

A point of general agreement is that the present geometry and internal structure of the orogen bears the stamp mark of a Miocene crustal extension, which was responsible for the opening of the western Mediterranean basin (Platt and Vissers, 1989; García-Dueñas et al., 1992). Pre-Miocene structures were strongly modified during this event, thereby complicating their recognition, correlation and interpretation using conventional field methods. We therefore investigated, for the first time in this orogen, the

* Corresponding author. Tel.: +34 958 242825; fax: +34 958 248527.
E-mail address: aerden@ugr.es (D. Aerden).

0191-8141/$ – see front matter © 2008 Elsevier Ltd. All rights reserved.
doi:10.1016/j.jsg.2008.06.009

kinematic archive constituted by porphyroblast inclusion trails in the Nevado-Filabride Complex (NFC), a garnet-rich high-pressure unit situated at the base of the Betic nappe stack (Fig. 1a,b). The detailed geometry and orientation of these microstructures will be shown to be closely related to macroscopic structural patterns in the study area, and to greatly facilitate their interpretation in a plate-tectonic context.

Research during the past two decades has revealed highly consistent orientations of inclusion trails in individual thin sections, folds and large metamorphic regions (e.g. Johnson, 1990; Hayward, 1992; Aerden, 1995, 1998, 2004; Bell et al., 1998; Bell and Mares, 1999; Jung et al., 1999; Timms, 2003; Cihan and Parsons, 2005; Sayab, 2005; Johnson et al., 2006; Yeh, 2007). Although some authors have attributed this to relatively coaxial deformation (Evins, 2005; cf. Ramsay, 1962), evidence for shearing and multiple folding histories has led the majority of workers to conclude that lack of porphyroblast rotation is a general consequence of the geometry of deformation-partitioning in metamorphic rocks (Bell, 1985; Aerden, 1995), recently modeled numerically by Fay et al. (2008). This model is also in better agreement with microstructural evidence demonstrating that spiral-shaped inclusion trails form by overgrowth of matrix crenulations instead of progressive porphyroblast rotation (e.g. Bell, 1985; Bell and Johnson, 1989; Hayward, 1992; Aerden, 1994, 1998; 2004; Stallard and Hickey, 2001 and references therein).

An important implication of a lack of (or limited) porphyroblast rotation is that included tectonic fabrics (i.e. inclusion trails) potentially conserved their original orientation in a reference frame fixed to bulk kinematic axes. For this reason, regionally consistent trends or strikes of inclusion trails have been, commonly, interpreted to record a direction of crustal shortening perpendicular to those trends, or changes therein with time. Our study provides a unique opportunity for testing these ideas via the comparison of deformation geometries across a large range of scales (porphyroblasts, samples, outcrops, cross-sections, maps) with the relative plate-motion history of the Mediterranean Alpine system. The latter is relatively well constrained by paleomagnetic data, contrary to most other (older) orogens where inclusion-trail orientations were quantitatively studied earlier.

2. Geological setting

2.1. The Betic–Rif orogen

The Betic–Rif orogen has been traditionally divided into an external fold- and thrust belt commonly referred to as "External Zones" (Fig. 1a,b) and its metamorphic hinterland or "Internal Zones". The former comprise Mesozoic to Tertiary passive-margin sediments, the latter deformed Variscan basement plus part of its Mesozoic cover. The External Zones were thrust onto their Iberian and North-African forelands during the Miocene, while the metamorphic hinterland experienced a simultaneous orogenic collapse following earlier mountain building (Platt and Vissers, 1989). Since the latest Miocene, renewed crustal shortening (Marín-Lechado

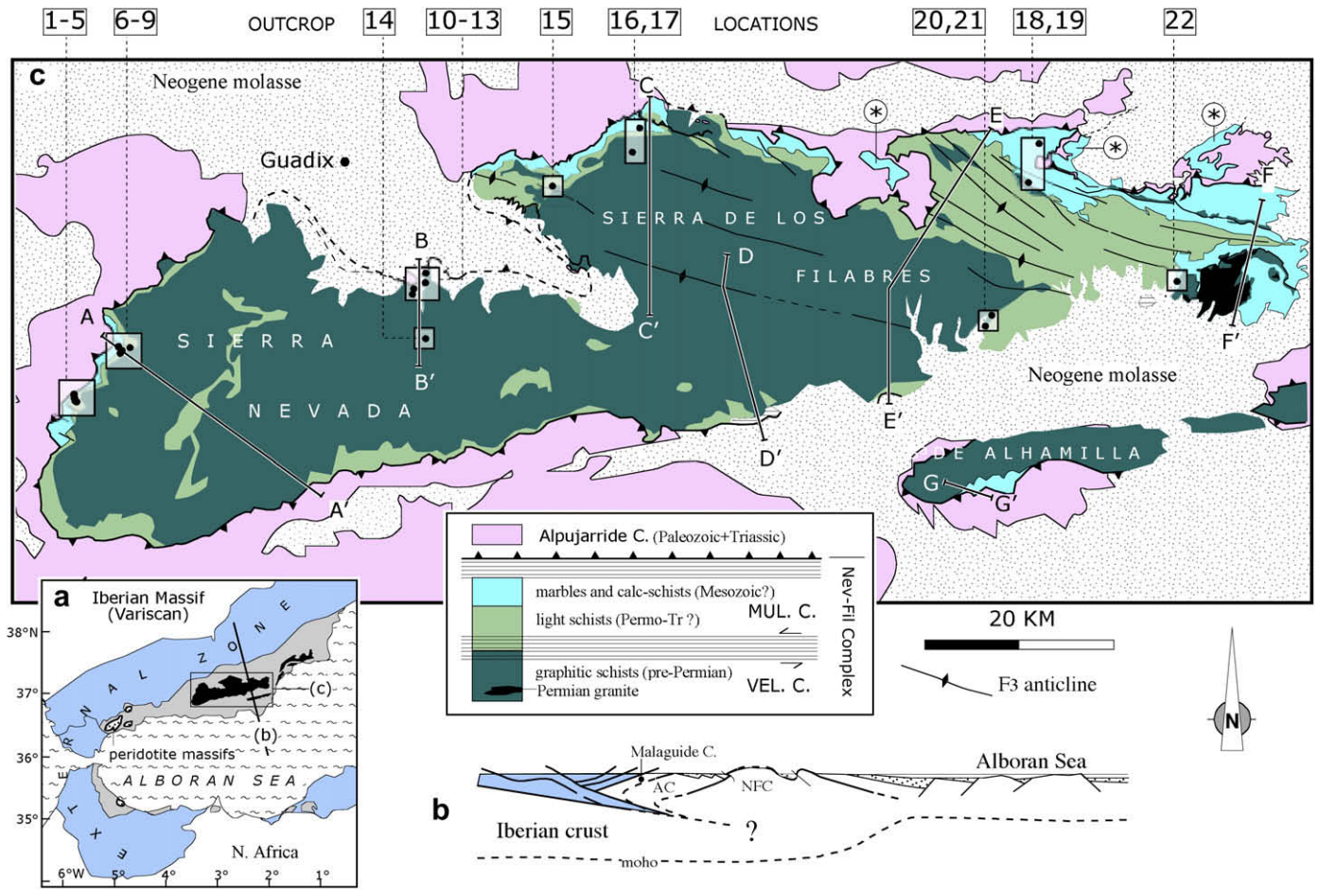

Fig. 1. (a) Simplified map of the Betic–Rif orogen with the Nevado-Filabride Complex (NFC) indicated in black. (b) Crustal cross-section through the orogen. (c) Geological map of the Nevado-Filabride Complex compiled after 1:50,000 national geological maps. Outcrop locations are numbered 1–22. Asterisk symbols along the northern boundary of Sierra de los Filabres indicate minor thrust imbrications that locally invert the Nevado-Filabride–Alpujarride positions.

et al., 2005) uplifted the peripheral parts of the previously extended Internal Zones and led to the development of a series of anticlines and synclines that control the present topography of "sierras" (ranges) separated by Neogene basins (Fig. 1c).

The Internal Zones have been subdivided in three nappe complexes, which are in ascending order the Nevado-Filabride, Alpujarride, and Malaguide Complexes. The latter has the most limited aerial extent and is only weakly affected by Alpine deformation. Consequently, low-grade Variscan structures are well preserved in the Palaeozoic series of this Ordovician to Miocene unit (Chalouan and Michard, 1990). By contrast, the two lower nappe complexes record Alpine high-pressure metamorphism and intense polyphase deformation. Both exhibit a similar lithostratigraphic column starting at the base with pre-Permian graphitic schists and quartzites locally intruded by late-Variscan granite (Zeck and Whitehouse, 2002), overlain by multi-colored metapelites and psamites of probable Permo-Triassic age, followed in turn by calcschists and marbles with intercalated metabasite lenses. The structural thicknesses of these three series in the NFC are in the order of 6, 2 and 1 km, respectively (Martínez-Martínez and Azañon, 1997). A Middle- to Late-Triassic age of the upper carbonaceous sequence has been established from fossils in the Alpujarride Complex, but remains controversial in the Nevado-Filabrides where depending on different structural interpretations, proposed ages range from Palaeozoic to Cretaceous (Puga et al., 2004b). The metabasite lenses, dated as Middle-Jurassic (Hebeda et al., 1980), have been interpreted as remnants of the Tethys ocean (Bodinier et al., 1987; Puga, 1990; Puga et al., 2002) or as plutonic bodies intruded in thinned continental crust (Gómez-Pugnaire et al., 2000).

The repeated lithostratigraphic columns of the three complexes as well as numerous internal thrust repetitions witness a major thrusting event. It is therefore not surprising that the main nappe contacts were interpreted as thrusts. However, more recent workers proposed their reinterpretation as late-orogenic extensional detachments, or thrusts reactivated as such (García-Dueñas et al., 1988; Galindo-Zaldivar et al., 1989; Jabaloy et al., 1993; Crespo-Blanc et al., 1994; Vissers et al., 1995; Martínez-Martínez et al., 2002; Augier et al., 2005b). Arguments for this include: (1) the presence of listric normal faults in the hangingwall of the contacts, (2) local gaps in metamorphic grade produced by the contacts, (3) excision of footwall stratigraphy in the direction of inferred movement along the contacts and (4) strong decompression during development of the main foliation in the complexes. Yet, the fact that the original nappe architecture of the Internal Zones is essentially preserved and of great lateral continuity is difficult to reconcile with an origin of the principal foliation and folds after the thrusting, as will be discussed further in Section 5.5.

2.2. The Nevado-Filabride Complex

The principal Nevado-Filabride outcrop is a 140 km long structural dome which comprises the Sierra Nevada and the Sierra de los Filabres (Fig. 1a,c). A two-fold subdivision of the complex was established by Brouwer (1926), Egeler and Simon (1969) and Puga et al. (1974) who recognized a more intensely deformed upper unit comprising a mixture of marbles, quartzites, metapelites and metabasite lenses, overlying a more monotonous and apparently less-deformed unit composed of Palaeozoic graphitic schists and quartzites. Both units are well known as the Mulhacen (above) and Veleta (below) complexes, which is broadly equivalent to the Bedar-Macael plus Calar-Alto Units and Ragua Unit of Martínez-Martínez et al. (2002). Due the scarcity of stratigraphic markers horizons in the NFC, internal tectonic contacts and shear zones have been mainly inferred indirectly from differences in metamorphic grade or deformation intensity. Consequently, the number and precise location of tectonic subunits remains controversial (González-Lodeiro et al., 2004).

Petrological studies have established a clockwise P–T–t path for the NFC with maximum pressures of about 2 GPa recorded by eclogite boudins (Puga et al., 2002 and references therein). Inclusion trails in garnets of metapelite rocks record somewhat lower pressure in the range of 10–15 kbar at 500–550 °C, which was followed by a near-isothermal decompression to about 3,5 kbar recorded by matrix assemblages (Nijhuis, 1964; Vissers, 1981; Bakker et al., 1989; Augier et al., 2005a). A late-stage reheating to more than 500 °C is witnessed by oligoclase rims of albite porphyroblasts and late staurolite and garnet growth (Vissers, 1981; Bakker et al., 1989; De Jong, 1993b).

Geochronological studies have furnished a large range of ages for the high-pressure metamorphism between 48 Ma or older and 17 Ma (e.g. Puga et al., 2004a; Augier et al., 2005a; Platt et al., 2006). In-situ ^{39}Ar–^{40}Ar dating of white mica associated with successive matrix fabrics (Augier et al., 2005a) situates development of the main cleavage between 30 Ma and 20 Ma (Late-Oligocene to Mid-Miocene), followed by detachments tectonics between 20 Ma and 10 Ma. Prograde metamorphism would have occurred prior to 30 Ma, coinciding with ages generally accepted for the Alpujarride Complex (Monie et al., 1994; Platt et al., 2005). However, recent Lu–Hf garnet ages between 18 and 14 Ma obtained by Platt et al. (2006) from four NFC samples, and interpreted as dating high-pressure conditions, sharply conflict with most of the earlier collected age data. Thus, either the Ar–Ar and K–Ar ages in the NFC are to old, or the Lu–Hf ages are to young as will be discussed further (Section 5.3).

3. Macroscopic structural sequence

Based on a careful review of the structural sequences and cross-sections of earlier workers (Fig. 2) and our new field evidence, we define five deformation phases in the NFC (D_1–D_5) that are described in the following sections. Their correlation with the deformation sequences of earlier workers is summarized in Table 1, and further discussed.

3.1. Main-phase deformation (D_1–D_2)

The NFC is characterized by a penetrative cleavage variably termed "regional foliation", "principal foliation", "main-phase foliation", "transposition foliation" or "plano-linear fabric" in the literature, which is axial-plane fabric of tight to isoclinal folds that reach km scale. Depending on lithology and the local intensity of deformation this foliation variably appears as a simple schistosity, a mylonitic foliation or a compositionally differentiated crenulation cleavage, in which case, an older fabric (S_1) is observed in microlithons. However, outcrop-scale F_1 folds have only be rarely identified.

3.2. NW to WNW upright folding (D_3)

A system of NW to WNW trending anticlines and synclines is prominently developed in the eastern Sierra de los Filabres (Fig. 1c) and associated with a steeply NE dipping to subvertical crenulation cleavage (S_3). The intensity of this deformation decreases towards the west and south, where F_3 folds are more open. In zones of most intense development, S_3 is morphologically indistinguishable from S_2, and this may explain why Jabaloy-Sánchez, 1993 and Vissers (1981) originally correlated F_3 folds in northern parts of their study areas with recumbent F_2 folds

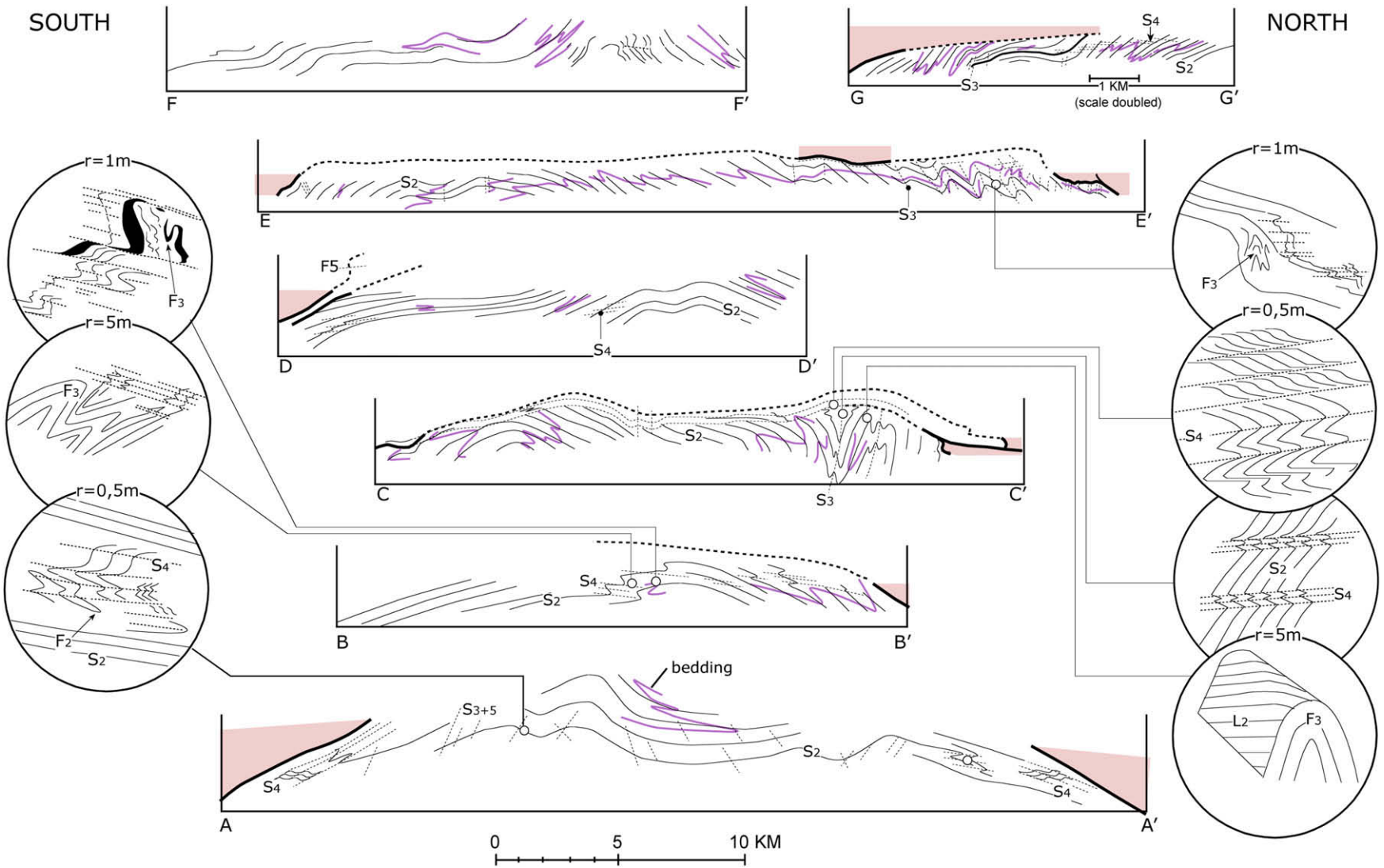

Fig. 2. Structural cross-sections based on or modified after Galindo-Zaldivar, 1993 (A–A′), own data (B–B′), Jabaloy-Sánchez, 1993 (C–C′), Martínez-Martínez, 1986a (D–D′), Vissers, 1981 (E–E′), Soto, 1991 (F–F′), and Platt and Behrmann, 1986 (G–G′). Cross-section lines are shown in Fig. 1c. Note opposite F_4 fold asymmetries on our new cross-section (B–B′) suggesting a component of vertical flattening (D_4) superposed on a pre-existing F_3 anticline. Upright folds in the northern parts of sections C–C′ and E–E′ have been reinterpreted as F_3 (see Section 3.2).

Table 1
(a) Deformation sequences defined by previous workers in the NFC ("x" stands for "D_x" etc.); (b) Suggested correlation of deformation phases shown in (a)

This study	Langenberg 1972	Kampschuur 1975	Vissers 1981	Jabaloy Sanchez 1993	Galindo Zaldivar 1993	Martínez Martínez 1986a	Bakker et al. 1989	DeJong 1993b	Platt & Behrmann 1986	Soto 1991	Augier 2005
1	1	1	h	r-1	pre-p	1	x-1	1	q	r	1
2	2	2	1	r	p	2	x	2	r	s	2
3	3	3	2	p	c	3	x+1(ecc)	3	s	t	3(ecc)
4	4	4	3	c	ecc	m	x+2	4	t	m	
5a	5	5	4	ecc		4	x+3	5(ecc)	u	u	
5b		6		n		5		6		post-u	
						6		7			
SUGGESTED CORRELATION											
1	1	1	h 1	r-1	pre-p	1	x-1	1	q	r	1
2	2	2 3	2	r c	p	2	x	2	r	s	2
3	3	5	3	c	c	5	x+3	4	u	t	
4		4	2r 4	p (=rr) c ecc	pr c ecc	m=2r 3	x+1 x+2	2r 3 5	rr s t	m=s r u	2r 3
5a	4	6	4	n		4		7	u	u	
5b	5		4	n		5 6		6		post-u	

The suffix "r" stands for "reactivation" and mylonitization of the main schistosity (S_2 in our scheme) during D_4. Our correlation implies that some structures and fabrics were mixed or incorrectly timed previously (discussed in Section 4).

further south. However, Bakker et al. (1989) and De Jong (1993b) noticed that the steep folds in the north (their "F_{x+3}" and "F_4" folds respectively, Table 1) deform the main cleavage, and we confirmed this along our new cross-section (Fig. 2, section B–B′) and the cross-sections of Jabaloy-Sánchez, 1993 and Vissers (1981), reinterpreted in Fig. 2 (sections C–C′ and E–E′).

3.3. Detachment-related deformation (D_4)

The Nevado-Filabride and Alpujarride complexes are separated by a major detachment fault variably termed "Betic Movement Zone" (Platt and Vissers, 1980), "Filabres Detachment" (García Dueñas et al., 1992), or "Mecina Detachment" (Jabaloy et al., 1993), but simply called "Nevado-Filabride–Alpujarride Contact" here (NFAC). The contact is demarcated by lenses of mylonitic and cataclastic carbonate rocks (carneoles) and quartz-feldspar mylonites of variable thickness, from a few meters to several tens of meters. A zone of associated ductile deformation extends several hundred meters further downward into the footwall, and is characterized by a subhorizontal crenulation cleavage, shear-band cleavage, and mesoscopic shear zones. Gradual transitions from normal ("compressional") to extensional crenulations in this zone suggest that both represent the same S_4 cleavage, instead of a progressive shear-zone fabric or ("S–C" fabric s.s.). This also explains why F4 crenulations (extensional or compressional) and associated mesoscopic F4 folds switch vergence between opposite limbs of (pre-existing) F3 folds (Fig. 2, section B–B′).

Mapping of the lower boundary of the regional D_4-strain zone, notably by Jabaloy-Sánchez (1993) (Fig. 2. section C–C′), plus a few minor Alpujarride klippen in the Sierra de los Filabres and Sierra de Alhamilla indicates a subhorizontal attitude of the NFAC prior to its erosion, and the truncation of upright F_3 folds by it (Fig. 2, sections B–B′ and C–C′). Although this overprinting relationship was recognized by some workers (Vissers, 1981; Bakker et al., 1989; De Jong, 1993b; Soto, 1991; Table 1), other workers rationalized it in terms of syn-D2 extensional ramps locally cutting S_2 cleavage (García-Dueñas et al., 1988; Martínez-Martínez et al., 2002).

3.4. Late- to post-Miocene folding and faulting (D_{5a}, D_{5b})

Several authors have reported a late set of upright folds with conspicuous N–S to NE–SW trends and an associated weak crenulation cleavage (here called D_{5a}). Martínez-Martínez et al. (2002) suggested an origin by extensional updoming of the footwall of an extensional detachment (i.e. the NFAC). However, the presence of similar structures and fabrics in the hangingwall of this contact ("S_{t-2}" of Platt et al., 1983), plus the vertical attitude of the associated crenulation cleavage make us favor an origin via moderate E–W to WNE–ESE compression.

The location of structural domes versus Neogene basins is controlled by late- to post-Miocene folding about roughly E–W trends and related faulting with major strike–slip components (Martínez-Martínez, 2006). This deformation (called D_{5b} here) is concentrated along basin edges where the NFAC is steepened,

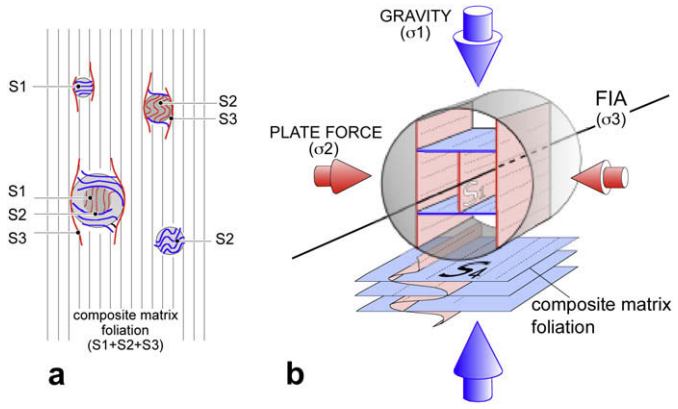

Fig. 3. (a) Conceptual model illustrating how variable inclusion-trail geometries can be formed during successive development of sub-orthogonal foliations (S_1 to S_3). (b) 3D sketch of multiple foliations within a single porphyroblast defining a Foliation-Intersection-Axis ("FIA"). The matrix contains a composite fabric that mixes four foliations. FIA are expected to form perpendicular to the direction of bulk shortening. If the least principal stress is parallel to FIA, stretching lineations will form parallel to FIA and fold axes.

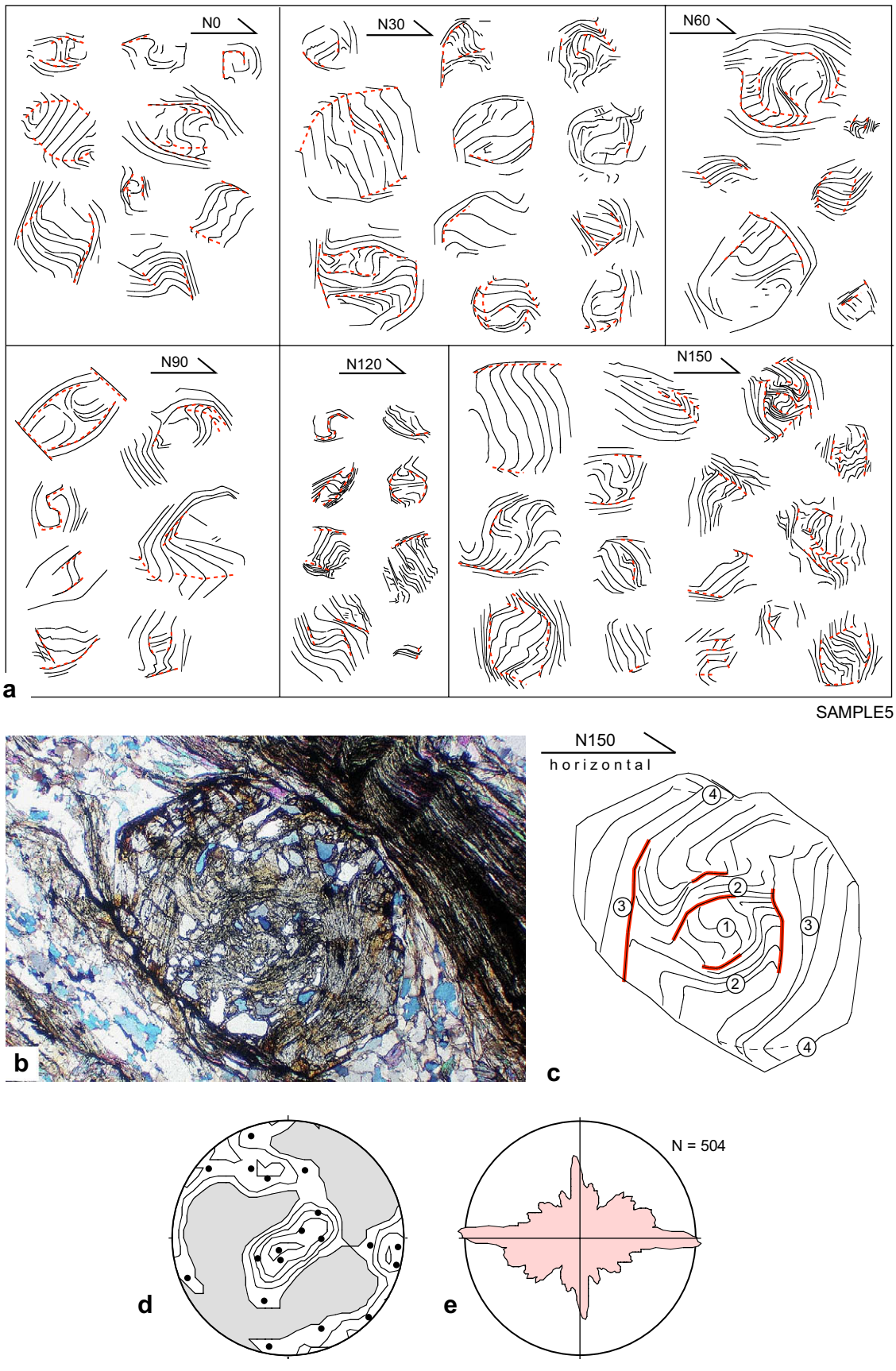

Fig. 4. (a) Accurate line tracings drawn on high-magnification microphotographs of all inclusion trails observed in six vertical thin sections with different strikes of sample 5. Half-arrows indicate horizontal and geographic trend. Stipple lines demarcate truncation surfaces and axial planes of inclusion trails. (b, c) Microphotograph and enlarged line tracing of one of the garnet porphyroblasts in the N150 thin section in (a). Numbers indicate the interpreted foliation sequence. (d) Poles of best-fit planes calculated with "FitPitch" for samples 1, 2a, 2b, 3c, 3b, 4a, 5 and 10 showing preferred horizontal and vertical orientations. See electronic supplement for details of this analysis. (e) Moving-area rose diagram ($\pm 10^{\circ}$ counting interval) plotting the orientations of all individual dashes of the dashed lines that mark truncations and axial planes in (a). Measurements were acquired automatically with the "NIH_Image" program.

locally overturned and even cut by thrusts placing NFC rocks on top of the Alpujarride Complex (Fig. 1c). Several authors have described weak crenulations and chevron folds associated with post-detachment deformation with variably oriented axial planes (Vissers, 1981; Martínez-Martínez, 1986a; De Jong, 1991). The significance and precise relative timing of these late fabrics remain to be established, as counts for the relative timing of D_{5a} versus D_{5b}.

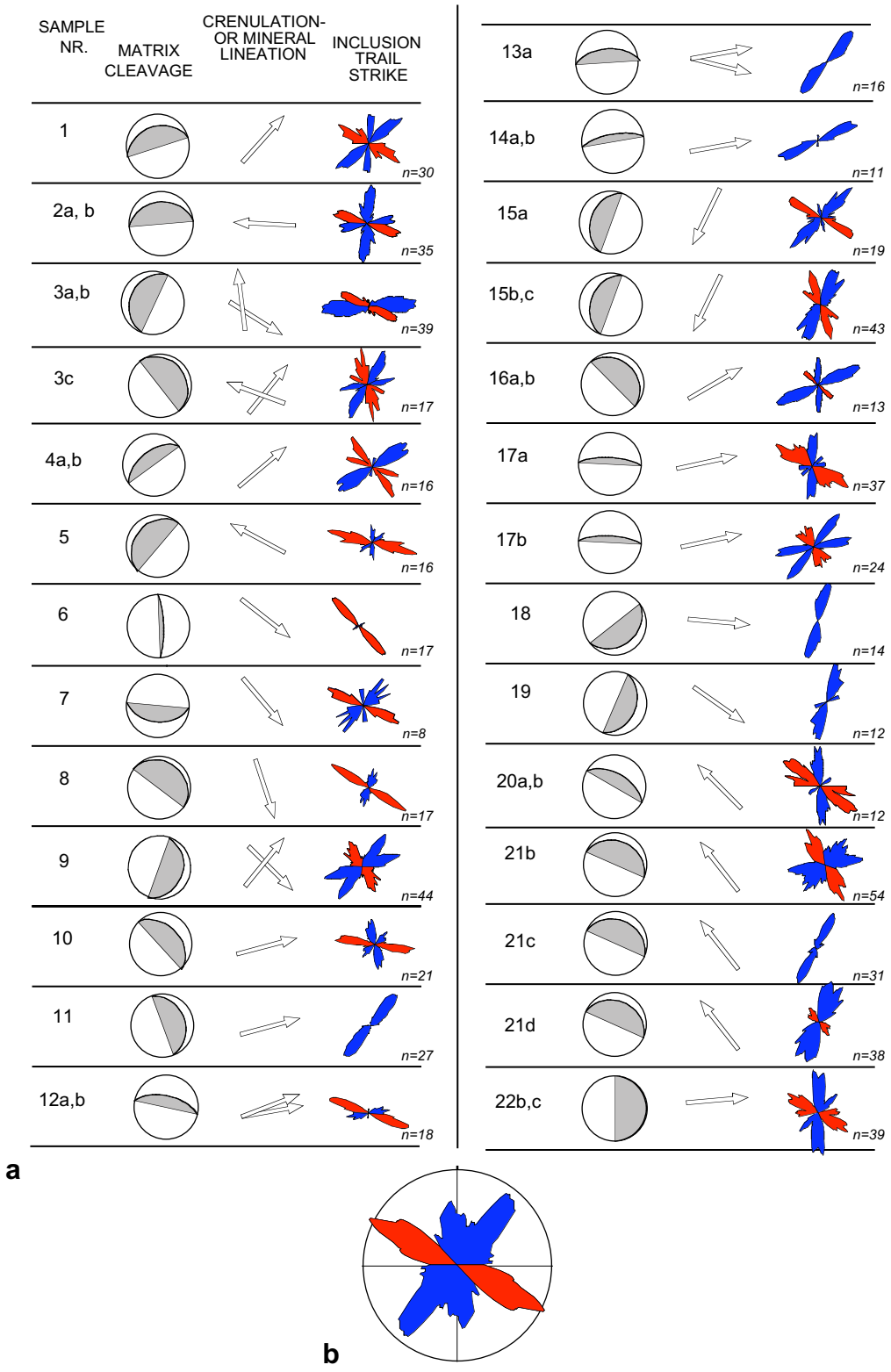

Fig. 5. (a) Chart showing the orientation of the macroscopic foliation and lineation in 36 analyzed samples, and the strike of inclusion trails (rose diagrams). Sample numbers match outcrop numbers in Fig. 1c. Multiple samples from the same outcrop with few porphyroblasts were in some cases combined (e.g. samples 4a and 4b). The data are interpreted to reflect the presence of two age groups of inclusion trails indicated blue and red. (b) Rose diagram re-plotting the modal peaks in (a) demonstrates the bimodal character of the orientation data. Rose diagrams were constructed using "Stereoplot" (N. Mancktelow) using a $\pm 10^{\circ}$ counting interval.

4. Inclusion-trail analysis

4.1. Sample description

Inclusion trails were analyzed from 36 garnet-schist samples collected from 22 outcrop locations (Fig. 1c). Samples from locations 11–14, plus 20 and 21 are quartz-rich graphitic schists from the Veleta Complex containing relatively small garnets (between 1 and 2 mm). The latter exhibit straight to weakly curved inclusion trails almost exclusively composed of graphite and quartz. The rest of the samples were gathered from the Mulhacen Complex and are characterized by larger garnets (typically between 2 and 10 mm) with more complex inclusion-trail patterns, commonly surrounded by a mylonitic matrix foliation. The mineralogy of the inclusion trails is also more variable, including quartz, graphite, rutile, ilmenite, plus minor amounts of cloritoid, staurolite, clinozoisite and kyanite.

4.2. Methodology

Hayward (1990) devised a method to determine the 3D orientation of the axes of inclusion-trail curvature in a sample, commonly referred to as "Foliation-Intersection Axes" in the literature (abbreviated as "FIA"; Fig. 3a,b). The technique consists in recording a switch in curvature asymmetry of inclusion trails

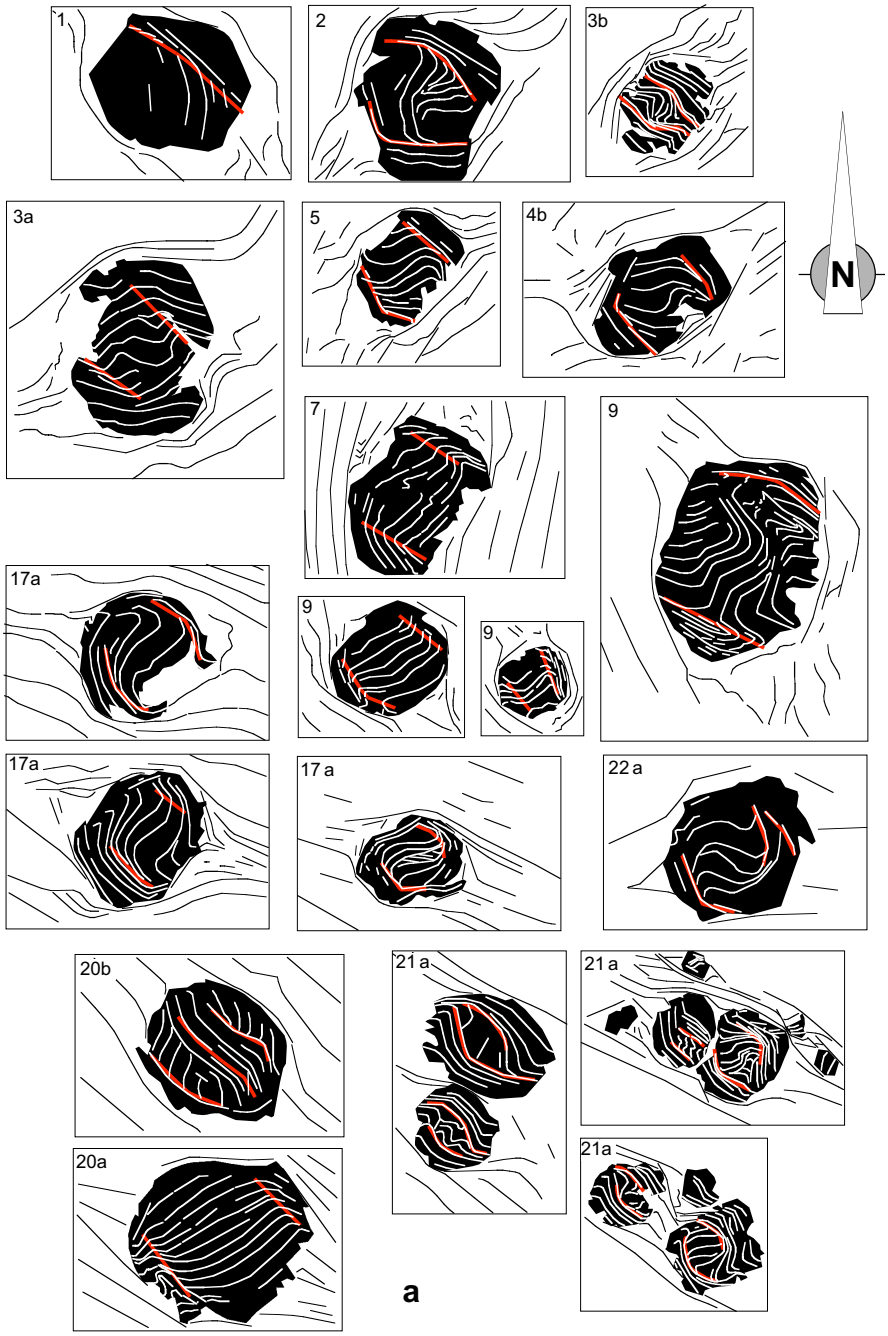

Fig. 6. (a, b) Accurate line tracings drawn on microphotographs of horizontal thin sections. Sample numbers are indicated in the top left corner of each frame. Garnets from the Mulhacen Complex samples (a) preserve NW foliations in rims and NE ones in cores. Garnet porphyroblasts in the Veleta Complex (b) have consistent NE trends and contain a NW trending crenulation cleavage in the matrix. (c) Accurate line tracing of folded quartz vein in sample 13c surrounded by numerous small garnet porphyroblasts (represented as dots) with consistently orientated inclusion trails (line segments). (d) Kinematic interpretation of (c).

(clockwise to anticlockwise) in series of vertical thin sections cut at different strike angles from a sample. Bell et al. (1995) refined the method to allow separate determination of FIA preserved in core versus rim zones of porphyroblasts. However, a prerequisite for the method is that inclusion trails exhibit consistent, or at least predominant, curvature senses in individual thin sections.

Unfortunately, this condition was not met by most of our NFC samples, which mostly exhibit roughly equal proportions of porphyroblasts showing opposite curvature asymmetry in thin section, or relatively symmetrical inclusion-trail patterns (e.g. Fig. 4a). Similar problems led Aerden (2003) to develop an alternative, numerical approach for studying inclusion trails in 3D. He wrote a computer program ("FitPitch") by which strike- and pitch-angles of inclusion trails measured on differently oriented thin sections of a sample, can be fitted, to one or multiple best-fit planes. Calculated best-fit planes define the preferred orientation of included foliations, and the intersection lines of such planes represent "FIA". The program assesses if data are best fitted to a single plane, a combination of two or three planes (single, bimodal or trimodal data) and quantifies the degree of fit in terms of standard deviation normalized by uniform data.

Wherever the asymmetry technique and the "FitPitch" method have been both applied to the same samples, their respective results have been found to be in excellent agreement (e.g. Aerden, 2004; Sayab, 2005). Significantly, modal maxima defined by the strike of inclusion trails have been generally found to match FIA trends independently established with the asymmetry method. Thus, strike measurements can be used as a proxy for FIA with the advantage of requiring much fewer thin sections. Consequently, our approach in the NFC was to measure strikes of inclusion trails in all porphyroblasts observed in all horizontal thin sections of all collected samples, and complement this data with more punctual observations from vertical sections of the same samples. Full 3D analysis (FitPitch) was only applied to 8 samples collected during an early stage of the research in the western part of Sierra Nevada.

4.3. Regionally consistent inclusion-trail orientations

Strike and pitch angles were measured for two types of inclusion trails, namely, (1) straight to weakly sigmoidal inclusion trails, and (2) truncation surfaces plus axial planes of more complex inclusion-trail patterns (Figs. 3a, 4a). The genetic relationships inferred between these elements are illustrated in Fig. 3a.

Rose diagrams for the strike measurements (Fig. 5a,b) exhibit a remarkable degree of consistency between the samples despite highly variable orientations of matrix fabrics and large distances between samples. A significant portion of samples yielded roughly bimodal strike patterns, which upon inspection of thin sections appeared to correspond to different age groups of inclusion trails. In almost every horizontal thin section from the Mulhacen Complex, at least some porphyroblasts were found preserving NW–SE trending inclusion trails in the rims enclosing roughly NE–SW trending trails in the cores, often separated by a sharp truncation (Fig. 6a). Vertical sections of the same samples revealed steep to subvertical dips of the rim trails (Fig. 7).

Samples from the Veleta Complex (Fig. 6b,c) contain simpler trails with highly consistent NE–SW strike. The matrix of these samples contains a steeply dipping NW–SE trending crenulation cleavage tentatively correlated as S_3 (Section 3.2). The older (crenulated) schistosity in the samples is continuous with, but oblique to the inclusion trails which we attribute to ductile matrix reorientation during D_3 relative to stable porphyroblasts (cf. Aerden, 1994, 1995).

Thus, the strike of inclusion trails in the Veleta samples matches the strike of porphyroblast-core trails in the Mulhacen Complex. On the other hand, the matrix crenulation cleavage in samples (S_3) of the Veleta Complex has a similar orientation as porphyroblast-rim trails in the Mulhacen Complex. Consequently, both pairs of fabrics are reasonably correlated as belonging to two sets of fabrics with distinctive trends and consistent relative timing in the study area, although we admit that this is a first-order classification that may need to be refined in the future. For example, a weak N–S modal

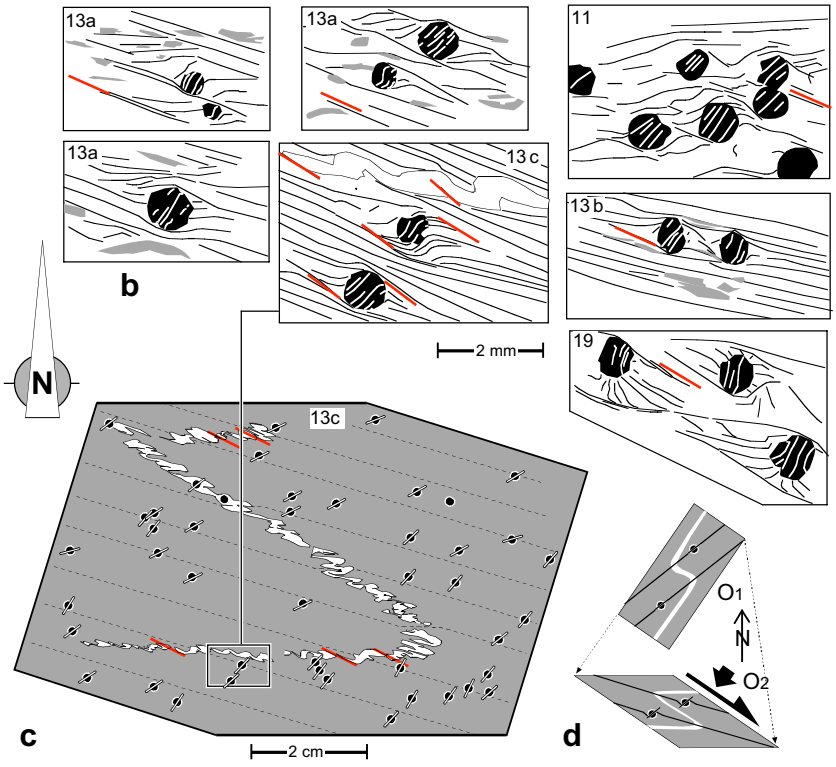

Fig. 6. (*continued*).

maximum is also apparent in Fig. 5b, whose significance is not clarified in this paper. Interestingly, our interpretation implies that garnet growth in the Veleta Complex ceased earlier as in the Mulhacen complex, where S_3 was still included in porphyroblasts.

As mentioned earlier, the "FitPitch" method (Aerden, 2003) was applied to eight samples from which six vertical thin sections spaced 30° around the compass, plus one or two horizontal sections were cut. Strike and pitch angles measured on all these sections were fitted to best-fit planes. The results of this analysis reveal vertical and horizontal preferred orientations of the inclusion-trail planes (Fig. 4d), consistent with direct observation (Fig. 4a–c) and computerized image analysis of 2D inclusion-trail patterns (Fig. 4e). The complete numerical output of the FitPitch analysis are provided as an electronic supplement to this article.

4.4. Correlation with macroscopic structures

Orientation patterns defined by inclusion trails in metamorphic regions can be partially mimicked by the trends of successive fold generations in the same regions (Aerden, 2004; Sayab, 2005), which greatly facilitated their correlation. With this experience in mind, a compilation was undertaken of all available orientation data for fold-axes and associated crenulation and/or mineral lineations in the NFC. Fold axes are generally subparallel to crenulation axes and mineral lineations in the NFC, although local overprinting relationships between oblique structures and fabrics have also been reported and observed by us (e.g. F_3 folding L_2). Over 8000 data were digitized from stereoplots or copied from data sheets, mainly corresponding to eight PhD theses (Langenberg, 1972; Vissers, 1981; Behrmann, 1982; Martínez-Martínez, 1986a; De Jong, 1991; Soto, 1991; Galindo-Zaldivar, 1993; Jabaloy-Sánchez, 1993). The data were represented in rose diagrams and placed in chronological order (Fig. 8a). Successive fabrics with statistically identical orientations were grouped together. The "$L_{S\text{-}C}$" data of Galindo-Zaldivar (1993) (subarea I, Fig. 8b) exclusively represent extensional crenulation axes, but we already argued in Section 3.3 why these fabrics can be treated equivalent to normal (compressional) crenulations.

Significant variation between the rose-diagram successions of different workers is thought to principally reflect the regional-scale heterogeneity of deformation with different folding phases more or less prominently developed in different subareas. However, additional variation stems from uncertain correlation of multiple fold generations that are difficult to discriminate in the field. For example, the principal foliation (S_2) drawn on the cross-sections A–A′ and C–C′ in Fig. 2 were originally interpreted as different fabrics

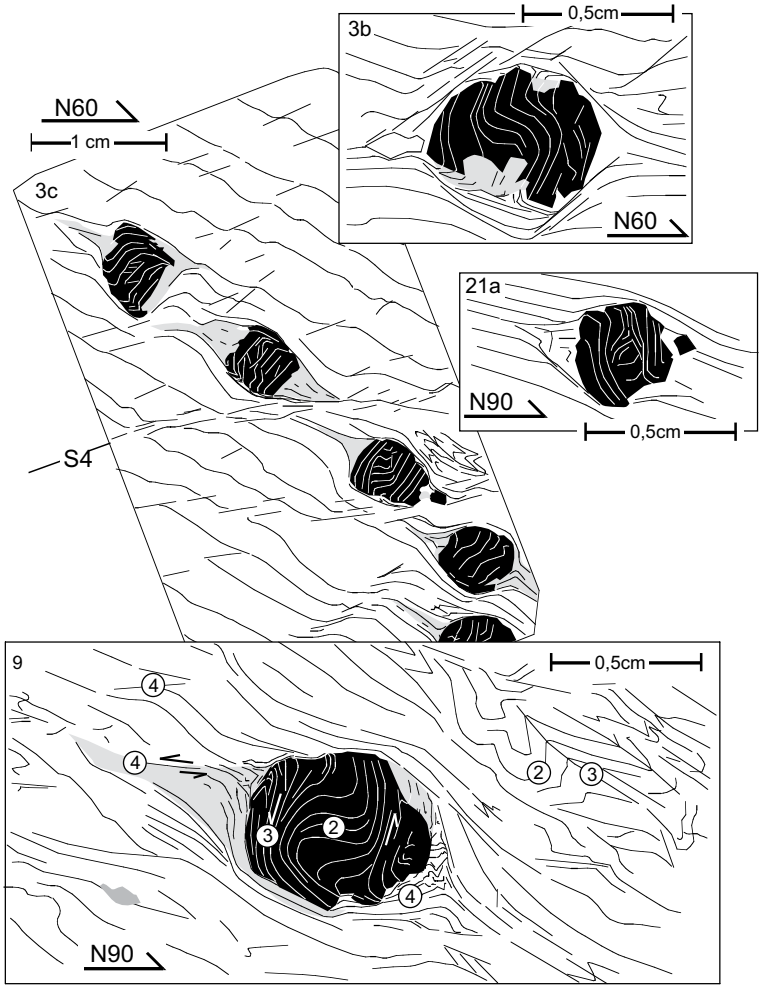

Fig. 7. Accurate line tracings drawn on microphotographs of inclusion trails from vertical thin sections of selected Mulhacen-Complex samples (sample numbers in top left corner of each frame). Half-arrows indicate horizontal and azimuth. Steeply dipping to subvertical inclusion trails in porphyroblast rims have NW trend when viewed on horizontal sections (Fig. 6a). Note opposite asymmetries of spirals in samples 3b and 3c, from the same outcrop. In sample 9, a top-to-the-west shearing component is indicated for S_4 by the asymmetry of (extensional) F_4 crenulations and the left porphyroblast strain shadows. This conflicts with a "snowball" interpretation of the spiral, but is consistent with the model illustrated in Fig. 3a.

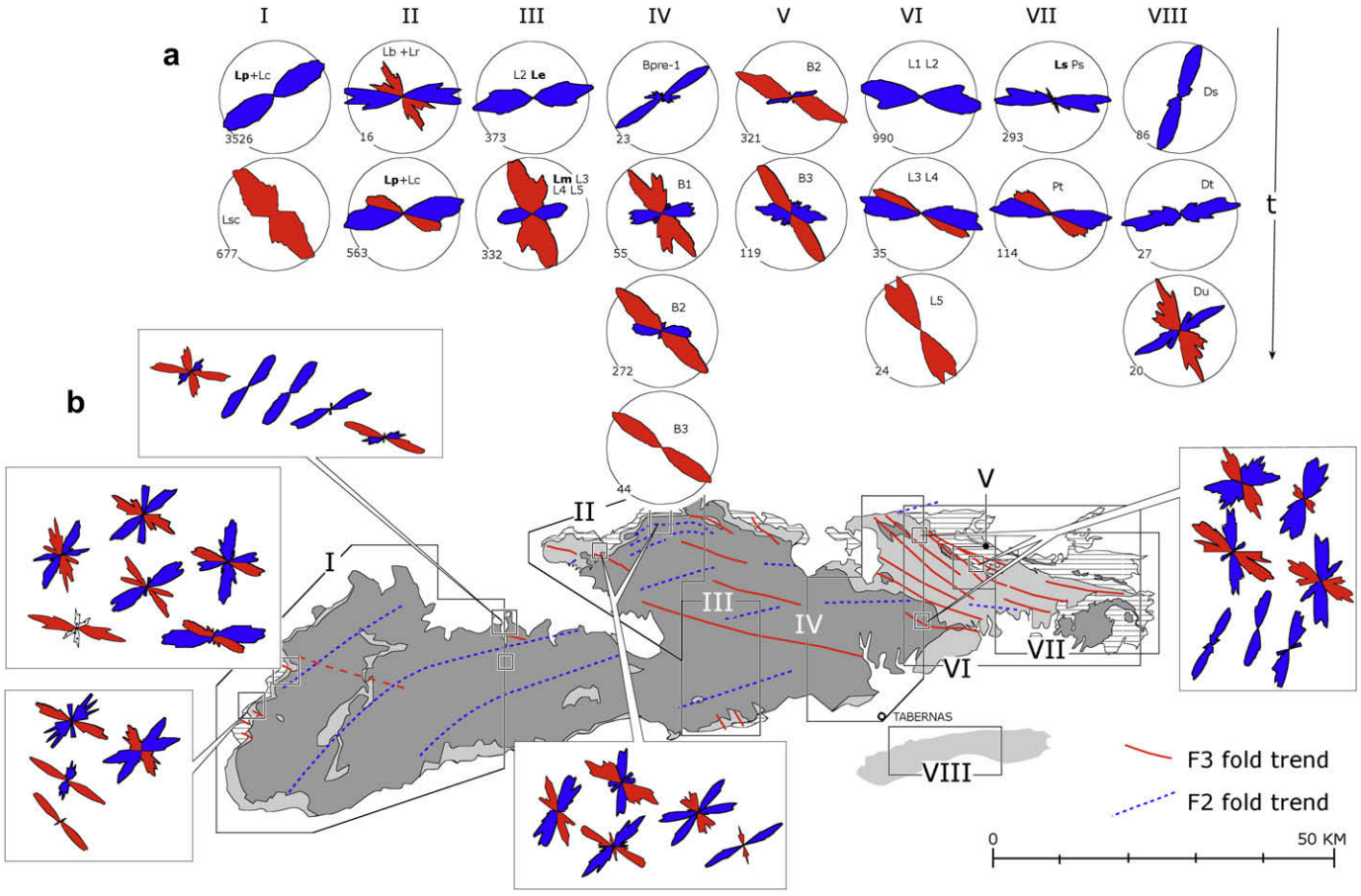

Fig. 8. (a) Rose diagrams plotting the trends of successive fold axes, crenulation axes and cogenetic mineral lineations measured by (I) Galindo-Zaldivar (1993), (II) Jabaloy Sánchez (1993), (III) Martínez-Martínez (1986a), (IV) Vissers (1981), (V) Langenberg (1972), (VI) De Jong (1991), (VII) Soto (1991) and (VIII) Platt and Behrmann (1986). The number of data and the original nomenclature are indicated in each plot. (b) Map showing the study areas of the above mentioned authors. Rose diagrams from Fig. 3a have been inserted to be compared with the field data in (a). Both data sets are compared further in Fig. 9.

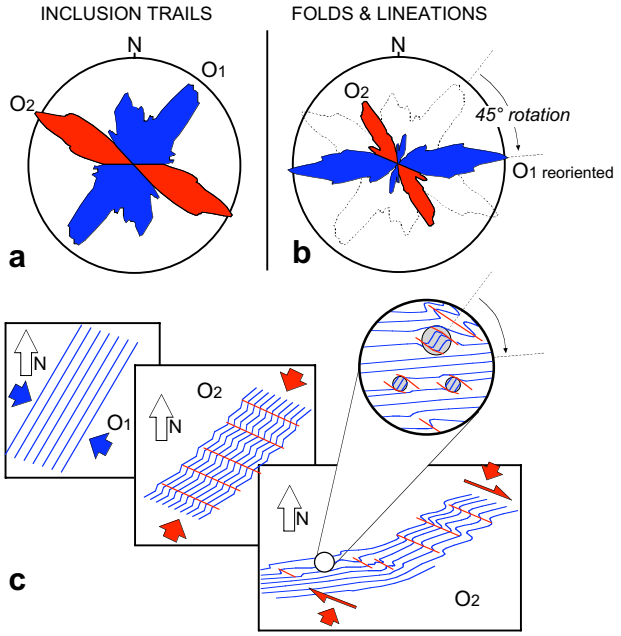

Fig. 9. (a) Rose diagram plotting all modal maxima in the rose diagrams of Fig 8b (inclusion trails). (b) Rose diagram plotting all modal maxima in the rose diagrams in Fig. 8a (filed data). See section 5.2 for discussion. (c) Conceptual kinematic model showing how O_1 trends were preserved in porphyroblasts while the matrix is reoriented.

(S_p and S_c, respectively; Table 1), but our intermediately located new cross-section (section B–B′) strongly suggests they are the same. Problems concerning the distinction of F_2 to F_5 folding phases were already described in Section 3. Finally, the composite nature of S_2 (e.g. Figs. 4a and 7), implies that F_2 folds could represent a mixture of different fold generations difficult to discriminate in the field as already acknowledged by earlier workers (Vissers, 1981; Platt and Behrmann, 1986; Soto, 1991).

Despite remaining uncertainty concerning the precise correlation of rose diagrams and modal peaks, an important coincidence can be noticed in the combined field data (Fig. 8a), namely, a progressive clockwise rotation of structural trends with decreasing age. The data from Vissers (1981) are most illustrative in this respect. His oldest recognized folds define a single NE–SW maximum. His subsequent folding phases ("F_1" and "F_2") show bimodal trends with a principal NW peak and a smaller E–W peak, which we interpret as originally NE–SW trending folds partially reoriented towards a younger NW–SE fold trend. The youngest fold generation ("F_3") exhibits a single NW–SE maximum. Similar progressions in the data of other workers remarkably match earlier described evidence for older NE–SW inclusion trails and younger NW–SE ones. In Fig. 9a,b the orientation maxima defined by folds and lineations versus inclusion trails are compared semi-quantitatively. The bimodal nature of both sets of data is clearly demonstrated in this Figure, but also an important misfit that will be interpreted in the next section.

5. Discussion and conclusion

5.1. Kinematic significance of the inclusion-trail pattern

Horizontal and vertical preferred orientations of inclusion trails as deduced here for the eight samples analyzed with FitPitch (Section 4.2) have been found earlier in many other orogens (Aerden, 2004 and references cited therein), and attributed to episodic porphyroblast growth punctuated by alternating crustal shortening and gravitational collapse (Bell and Johnson, 1989; Hayward, 1992; Fig. 3a). Cross-sectional geometries in the NFC are consistent with a succession of steeply dipping (S_3, S_5) and subhorizontal foliations (S_2, S_4), where as the inclusion trail record allows to extend this cyclicity further back in time (Figs. 4a–c, 7).

Shortening-collapse cycles can be expected to heterogeneously affect an orogen, and produce variable structural successions at different locations. However, as long as the direction of crustal shortening remains constant, foliations can be expected to all form about a common axis (Fig. 3b). For this reason, regionally consistent FIA trends have been generally interpreted to record crustal shortening perpendicular to that trend. The two sets of inclusion trails recognized in the NFC would thus indicate two successive orogenic stages (O_1 and O_2 in further discussion) characterized by NW–SE and NE–SW shortening, respectively, although periodically interrupted by second-order phases of gravitational collapse. The fact the stretching lineations are generally parallel to fold axes in the NFC can be explained assuming that contraction-collapse cycles resulted from permutations between the maximum and intermediate stress axes (σ_1 and σ_2), while the least principal stress (σ_3) consistently remained horizontal (Fig. 3b). In the next sections we will show that a two-stage orogenic evolution is not only consistent with regional-scale structural patterns in the NFC, but also makes sense when considering the plate-tectonic history of the Mediterranean Alpine system.

5.2. Fold trends and regional lineation pattern in the NFC

The regional pattern defined by mineral lineations, crenulation axes and fold axes in the NFC (Fig. 10a) has been variably interpreted in terms of (1) a continuously curving arc of unknown significance (Jabaloy et al., 1993), a superposition of different tectonic transport directions (Martínez-Martínez, 1986b; Martínez-Martínez and Azañon, 1997), and a divergent flow during core-complex formation (Augier et al., 2005a). Our interpretation is affine to the model of Martínez-Martínez (1986b) insofar as a succession of two orogenic stages is assumed. Fig. 10b illustrates how progressive reorientation of originally NE trending folds and lineations (O_1) during their overprinting by NW trending ones (O_2) readily explains the observed variation in orientations. The sense and amount of reorientation can be deduced from the difference in trend of O_1 inclusion trails versus O_1 in the matrix (Fig. 9a,b): approximately 45° clockwise.

In the Mulhacen Complex of the western Sierra Nevada we newly identified extensive areas with anomalous NW–SE trending mineral lineations and fold axes, developed at right angles to consistent NE–SW lineations in the Veleta Complex below. Overprinting relationships between both trends were locally observed in outcrop. A similar situation was reported by Martínez-Martínez (1986a) who found ENE–WSW lineations in the Veleta Unit progressively changing to bimodal orientations in the Mulhacen Complex with a principal NNW–SSE peak (Fig. 8a, subarea III). These contrasting fabric orientations suggest a late tectonic contact (D_4) between the two complexes that transported rocks intensely affected by O_2-related deformation (NW–SE trends) on top of rocks only weakly affected by this deformation (Fig. 11b,c), and associated reorientation.

We cannot offer a unique explanation for the smaller difference (approximately 20°) between the strike maximum of O_2 inclusion trails versus O_2 in the matrix (Fig. 9c,d). One possibility is that the direction of crustal shortening during O_2 was not constant but gradually rotated clockwise. Another possibility is that the matrix experienced additional vorticity-induced reorientation (relative to porphyroblasts) during a third orogenic stage (O_3) characterized by NW–SE Africa–Eurasia convergence and continuing today (see next section).

5.3. Links with vectors of relative plate motion

To assess the possible significance of two orogenic stages (O_1 and O_2) postulated above within the plate-tectonic context of the western Mediterranean region, a series of paleogeographic maps were constructed using the interactive plate-reconstruction tool of the Ocean Drilling Stratigraphic Network (ODSN; www.odsn.org). Maps were constructed in 5 Ma increments covering the last 55 Ma with the position of Iberia kept fixed. Paleogeographic maps for selected time frames (50, 30, and 20 Ma; Fig. 11) were complemented with data from Lonergan and White (1997), Faccenna et al. (1997), Michard et al. (2002) and Schettino and Turco (2006). The trajectory of Africa relative to Iberia according to this reconstruction includes a period of relatively stable NNE to NE convergence between 35 Ma and 20 Main agreement with earlier studies (e.g. Dewey et al., 1989; Rosenbaum et al., 2002). Prior to 35 Ma, the trajectory is more irregular and corresponded to a period of mainly transcurrent Africa–Iberia motion (Azores transform), possibly with a brief period of divergence between 45 and 35 Ma. Orogenic activity during this time was concentrated in a roughly NE–SW trending belt bordering "Greater Iberia" (including Sardinia–Corsica) and probably continuing in the Alps (Briançonnais domain; Michard et al., 2002), in response to NW–SE convergence between Adria, the Liguride–Piemonte ocean and Eurasia. The trend of this precursor orogen coincides with that of our older recognized set of inclusion trails (O_1). We contend that for reasons already outlined in Section 1, the porphyroblasts hosting these microstructures were not rotated during subsequent ductile deformation and reorientation of the surrounding matrix (Fig. 6b–d).

Around 35 Ma, a transition from transcurrent to convergent Africa-Eurasia relative motion, or in other words, from Adria- to Africa-driven orogenesis ocurred, which explains the overprinting of O_1 by O_2 structures and fabrics. Ar–Ar ages between 30 Ma and 20 Ma for the main foliation in the NFC (e.g. Augier et al., 2005a) are consistent with garnet growth having recorded the O_1–O_2 transition. However, our model conflicts with the Lu–Hf garnet ages of Platt et al. (2006) between 18,2 Ma and 13,6 Ma as these suggest that prograde metamorphism was initiated well after 35 Ma. These authors argued that previous Ar–Ar and K–Ar ages for the NFC could have been affected by excess Ar and therefore be to old. However, before accepting this explanation, a number of questions need to be resolved first. For example, why would excess Ar have profoundly affected the NFC, but not the overlying Alpujarride Complex for which similar Ar–Ar ages as in the NFC are accepted (e.g. Platt et al., 2005)? Secondly, considering the microstructural evidence for multiple stages of garnet growth from syn-D_1 to late-syn D_3 (Bakker et al., 1989), what is the relative timing of the dated garnet fragments? Finally, can the authors exclude methodological problems that possibly produced to young Lu–Hf ages? For example, a potential problem with Lu–Hf dating is the presence of very small and therefore difficult-to-detect micro-inclusions of zircon (Scherer et al., 2000; Dempster et al., 2008) in the matrix and/or the garnets. Thus, we believe that more work is required to resolve discrepancies between ages obtained with different dating methods, before these ages can be used as definite constraints on the tectono-metamorphic evolution. We welcome initiatives aimed

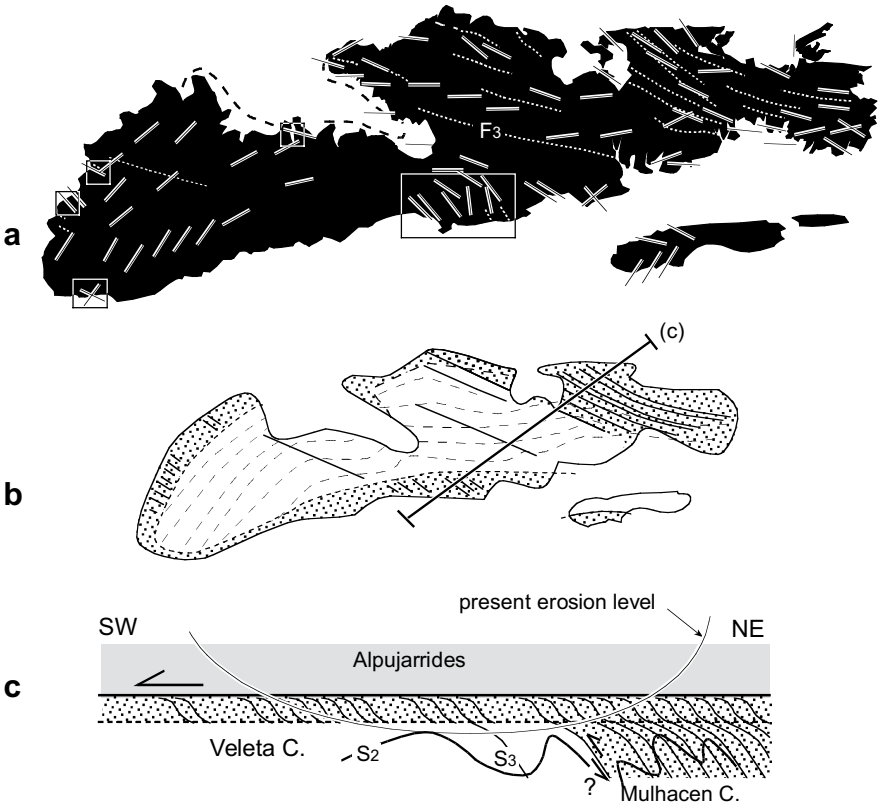

Fig. 10. (a) Compilation of dominant mineral lineation trends in the NFC. Boxes identify areas with bimodal mineral lineations. (b) Conceptual map-view interpretation of the lineation pattern in (a). (c) Conceptual cross-section (not to scale) along the profile line in (b). Contrasting fabric orientations of in the Mulhacen versus Veleta complexes are atributed to a late detachment placing rocks intensely affected by O_2 deformation and associated reorientation, on top of less affected rocks.

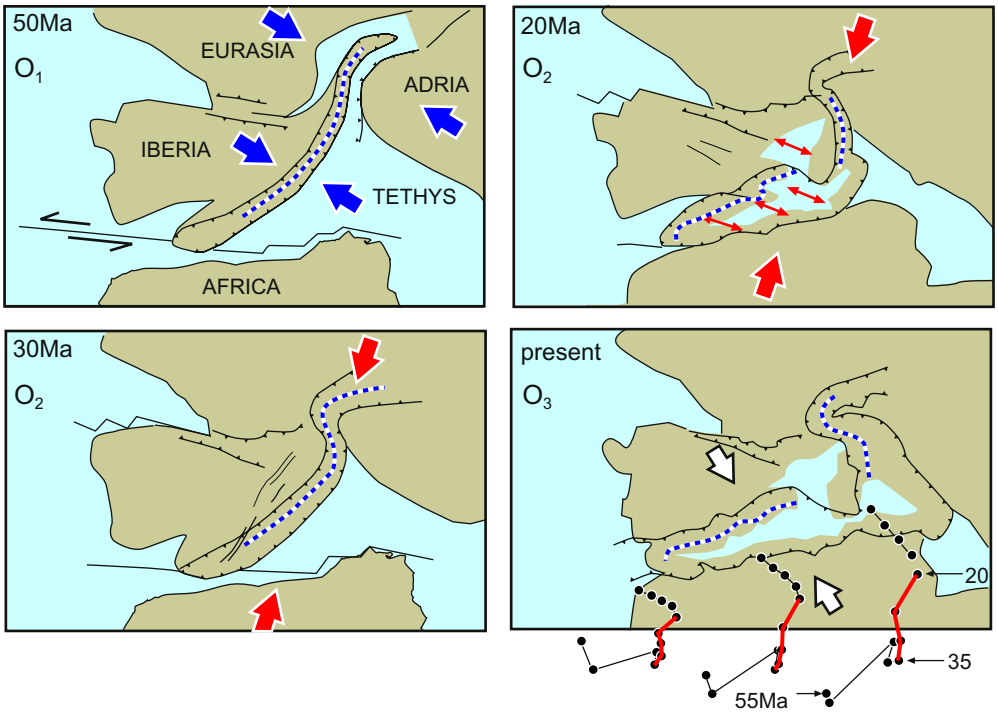

Fig. 11. Plate-tectonic evolution of the western Mediterranean region based on the online plate-reconstruction tool of the Ocean Drilling Stratigraphic Network. The trajectories of three points on the North-African margin relative to Iberia are indicated in the last time frame (present). Maps were refined using data from Faccenna et al. (1997), Michard et al. (2002) and Schettino and Turco (2006). A change from NW directed Adria–Iberia convergence, to NNE–SSW Africa–Iberia convergence is indicated around 35 Ma. See section 5.3 for discussion.

at dating the two sets of inclusion trails and hosting garnet phases described in this paper, and have already started a similar study as reported here for the NFC in the Alpujarride Complex and equivalent units in North Africa, which we hope will further contribute to unraveling the kinematics of this portion of the Alpine orogen.

5.4. Links with mantle processes and orocline formation

The coincidence in time of the transition from O_1 to O_2 and the onset of crustal extension in the western Mediterranean (Late-Oligocene) suggests a causal relationship. We contend that the waning of NW–SE oriented maximum stresses due to Adria–Eurasia convergence, and their progressive replacement by an almost perpendicular compression direction (Africa–Eurasia convergence) was what triggered the detachment and sinking of a lithospheric root, or the roll-back of a subducted slab, and the ensuing Miocene crustal extension (e.g. Michard et al., 2002). According to our paleogeographic reconstruction (Fig. 11), crustal extension was oriented perpendicular to NNE Africa–Iberia convergence, but strongly heterogeneous leading to the development of minor transform faults and oroclinal bending (Gibraltar Arc, Calabrian Arc, Western Alps). At some stage between 20 Ma and15 Ma, a second transition took place from NNE-SSW to the NW–SE oriented Africa–Iberia convergence that could be responsible for the D_{5a} structures described in section 3.4.

5.5. Is the NFC an extensional core complex?

Since the recognition of syn- or late-orogenic extension in mountain belts, many metamorphic domes previously interpreted as formed by crustal shortening and/or diapirism have been reinterpreted as extensional core complexes. In some cases, however, detailed study of the internal structure of such domes led to a partial rehabilitation of the role of contraction (e.g. Aerden, 1994, 1998; Aerden and Malavieille, 1999; Yeh, 2007). We contend that core-complex interpretations for the NFC also require a critical reassessment with particular attention to the following points.

(1) Core-complex models have simplified the internal structure of NFC to a subhorizontal foliation cut by low-angle normal faults with ramp-flat geometry (García Dueñas et al., 1992; Jabaloy et al., 1993; Martínez-Martínez and Azañon, 1997; Martínez-Martínez et al., 2002). The truncation of upright F_3 anticlines and synclines by the NFAC, and evidence for episodes of vertical foliation development are not considered. Consequently, the westward reduction in thickness of the higher sequence of the NFC (Fig. 1c) has been commonly rationalized in terms of a low-angle normal fault cutting a subhorizontal lithostratigraphy. Alternatively, however, a horizontal detachment (either extensional or thrust) could be considered cutting an inclined lithostratigraphy due to the effects of earlier upright folding and thrusting (Figs. 2, 10b,c).

(2) Stretching lineations and shear-sense criteria have been claimed to indicate progressive top-to-the-W shearing without much attention to conflicting shear senses, large spatial variation in the orientation of lineations (Fig. 10), and detailed fabric overprinting relationships. This complexity is well reflected in the large variety of tectonic transport directions proposed earlier in the NFC, including top-to-the-S followed by -N (Vissers, 1981), top-to-the-N followed by -S (Platt et al., 1983), top-to-the-E followed by -W (Martínez-Martínez, 1986a, b), top-to-the-W (García-Dueñas et al., 1992); top-to-the-SW (Jabaloy et al., 1993), top-to-the-S (De Jong, 1993a, b), or top-to-the-NNW followed by -WSW (Martínez-Martínez and Azañon, 1997).

(3) Normal faulting in the hangingwall of the NFAC (Crespo-Blanc et al., 1994; Vissers et al., 1995; Martínez-Martínez and Azañon, 1997; Orozco et al., 1998) and evidence for vertical shortening during D_4 are compatible with a low-angle extensional detachment. However, alternative crustal-strain geometries need to be considered as well, including a horizontal decollement separating zones with contrasting styles or intensity of deformation, or a thrust accommodating gravitational spreading in the hangingwall (Platt et al., 1983; cf. Aerden, 1998; Aerden and Malavieille, 1999).

(4) Petrological evidence for rapid decompression during development of the main cleavage (S_2) has been used to support an extensional origin of this foliation, but does not exclude exhumation realted to thrusting (e.g. Aerden, 1998; Stípská et al., 2004; Konstantinovskaya and Malavieille, 2005). The latter would certainly be easier to reconcile with the general nappe architecture of the Internal Zones. Finally, gaps in metamorphic grade can be produced by extensional detachment or thrusts depending on the pre-existing geometry of isograds, unknown in this case.

Acknowledgements

This study was funded by a grant from the Spanish Ministry of Education and Science. M.S. acknowledges financial assistance from the University of Granada during a work visit to Granada in 2006. We thank F. González Lodeiro, J. Galindo-Zaldivar, J.M. Martínez-Martínez, E. Puga, G. Booth, A. Jabaloy, and J.I. Soto for sharing their experience in the study area with us and discussion of their work. We thank Luiz Fernando Grafulha Morales and an anonymous referee for thoughtful comments that led to considerable improvement of the manuscript, and J. Hippertt for his editorial handling.

Appendix A. Supplementary data

Supplementary data associated with this article can be found in the online version, at doi:10.1016/j.jsg.2008.06.009.

References

Aerden, D.G.A.M., 1994. Kinematics of orogenic collapse in the Variscan Pyrenees deduced from microstructures in porphyroblastic rocks from the Lys–Caillaouas Massif. Tectonophysics 236, 139–160.
Aerden, D.G.A.M., 1995. Porphyroblast non-rotation during crustal extension in the Variscan Pyrenees. Journal of Structural Geology 17, 709–726.
Aerden, D.G.A.M., 1998. Tectonic evolution of the Montagne Noire and a possible orogenic model for syn-collisional exhumation of deep rocks, Hercynian belt, France. Tectonics 17, 62–79.
Aerden, D.G.A.M., 2003. Preferred orientation of planar microstructures determined via statistical best-fit of measured intersection-lines: the "FitPitch" computer program. Journal of Structural Geology 25, 923–934.
Aerden, D.G.A.M., 2004. Correlating deformations in the Iberian Massif (Variscan belt) using porphyroblasts; implications for the development of the Ibero-Armorican Arc. Journal of Structural Geology 26, 177–196.
Aerden, D.G.A.M., Malavieille, J., 1999. Origin of a large-scale fold nappe in the Montagne Noire (Variscan Belt, France). Journal of Structural Geology 21, 1321–1333.
Augier, R., Jolivet, L., Robin, C., 2005a. Late Orogenic doming in the eastern Betic Cordilleras: Final exhumation of the Nevado-Filabride complex and its relation to basin genesis. Tectonics 24, TC4003, doi:10.1029/2004TC001687.
Augier, R., Agard, P., Monie, P., Jolivet, L., Robin, C., Booth-Rea, G., 2005b. Exhumation, doming and slab retreat in the Betic Cordillera (SE Spain): in situ 40Ar/39Ar ages and P–T–d–t paths for the Nevado-Filabride complex. Journal of Metamorphic Geology 2005 (23), 357–381.
Bakker, H.E., de Jong, K., Helmers, H., Biermann, C., 1989. The geodynamic evolution of the Internal Zone of the Betic Cordilleras (SE Spain): a model based on structural analysis and geothermobarometry. Journal of Metamorphic Geology 7, 359–381.
Behrmann, J.H., 1982. Structures and deformational processes in a zone of contact strain beneath a nappe, Sierra de Alhamilla, Spain. PhD Thesis. University of Oxford, 99 pp.
Bell, T.H., 1985. Deformation partitioning and porphyroblast rotation in metamorphic rocks: A radical reinterpretation. Journal of Metamorphic Geology 3, 109–118.
Bell, T.H., Johnson, S.E., 1989. Porphyroblast inclusion trails: the key to orogenesis. Journal of Metamorphic Geology 7, 279–310.

Bell, T.H., Mares, V., 1999. Correlating deformation and metamorphism around orogenic arcs. American Mineralogist 84, 1727–1740.
Bell, T.H., Forde, A., Wang, J., 1995. A new indicator of movement direction during orogenesis—measurement technique and application to the Alps. Terra Nova 7, 500–508.
Bell, T.H., Hickey, K.A., Upton, G.J.G., 1998. Distinguishing and correlating multiple phases of metamorphism across a multiply deformed region using the axes of spiral, staircase, and sigmoidally curved inclusion trails in garnet. Journal of Metamorphic Geology 16, 767–794.
Bodinier, J.L., Morten, L., Puga, E., Díaz-de-Federico, A., 1987. Geochemistry of metabasites from the Nevado–FilabrideComplex, Betic Cordilleras, Spain: relics of a dismemberedophiolitic sequence. Lithos 20, 235–245.
Brouwer, H.A., 1926. Zur Tektonik der Betischen Kordilleren. Geologische Rundschau 17, 332–336.
Chalouan, A., Michard, A., 1990. The Ghomarides nappes, Rif coastal range, Morocco: a variscan chip in the Alpine belt. Tectonics 9, 1565–1583.
Cihan, M., Parsons, A., 2005. The use of porphyroblasts to resolve the history of macro-scale structures: an example from the Robertson River Metamorphics, North-Eastern Australia. Journal of Structural Geology 27, 1027–1045.
Crespo-Blanc, A., Orozco, M., Garcia-Dueñas, V., 1994. Extension versus compression during the Miocene tectonic evolution of the Betic chain; late folding of normal fault systems. Tectonics 13, 78–88.
De Jong, K., 1991. Tectonometamorphic Studies and Radiometric Dating in the Betic Zone (SE Spain) with Implications for the Dynamics of Extension and Compression in the Western Mediterranean Area. PhD Thesis. Vrije Universiteit, Amsterdam, 204 pp.
De Jong, K., 1993a. Large scale polyphase deformation of a coherent HP/LT metamorphic unit: the Mulhacen Complex in the eastern Sierra de los Filabres (Betic Zone, SE Spain). Geologie en Mijnbouw 71, 327–336.
De Jong, K., 1993b. Redefinition of the deformation scheme of the Mulhacen Complex and implications for the relative timing of the overthrusting of the Alpujarride Complex in the Betic Zone (SE Spain). Geologie en Mijnbouw 71, 317–326.
Dempster, T.J., Hay, D.C., Gordon, S.H., Kelly, N.M., 2008. Micro-zircon: origin and evolution during metamorphism. Journal of Metamorphic Geology 26 (5), 499–507.
Dewey, J.F., Cande, S., Pitman, W.C., 1989. Tectonic evolution of the India Eurasia collision zone. Eclogae Geologicae Helvetiae 82, 717–734.
Egeler, C.G., Simon, O.J., 1969. Sur la tectonique de la Zone bétique (cordillères bétiques, Espagne). Verhandelingen van de Koninklijke Nederlandse Academie voor Wetenschap 25 (90 pp.).
Evins, P.M., 2005. A 3D study of aligned porphyroblast inclusion trails across shear zones and folds. Journal of Structural Geology 27 (2005) 1300–1314.
Faccenna, C., Mattei, M., Funiciello, R., Jolivet, L., 1997. Styles of back-arc extension in the Central Mediterranean. Terra Nova 9, 126–130.
Fay, C., Bell, T.H., Hobbs, B.E., 2008. Porphyroblast rotation versus nonrotation: Conflict resolution!. Geology 36, 307–310.
Galindo-Zaldivar, J., 1993. Geometría de las Deformaciones Neógenas en Sierra Nevada (Cordilleras Beticas). PhD Thesis, Universidad de Granada, 249 pp.
Galindo-Zaldivar, J., González-Lodeiro, F., Jabaloy, A., 1989. Progressive extensional shear structures in a detachment contact in the western Sierra Nevada (Betic Cordilleras, Spain). Geodinamica Acta 3 (1), 73–85.
García-Dueñas, V., Martínez-Martínez, J.M., Orozco, M., Soto, J.I., 1988. Plis nappes, cisaillements syn- à post-métamorphiques et cisaillements ductiles-fragiles en distension dans les Névado-Filabrides (Cordillères bétiques, Espagne). Comptes Redues de lAcademie des Sciences Série 2 (307), 1389–1395.
García-Dueñas, V., Balanyá, J.C., Martínez-Martínez, J.M., 1992. Miocene extensional detachments in the outcropping basement of the northern Alboran Basin and their tectonic implications. Geo-Marine Letters 12, 88–95.
Gómez-Pugnaire, M.T., Ulmer, P., Lopez-Sanchez-Vizcaino, V., 2000. Petrogenesis of the mafic igneous rocks of the Betic Cordilleras: A field, petrological and geochemical study. Contributions to Mineralogy and Petrology 139, 436–457.
González-Lodeiro, 2004. Codilleras Beticas, Estructura. In: Vera, J.A. (Ed.). Geología de España, Madrid, pp. 427–429.
Hayward, N., 1990. Determination of early fold axis orientations in multiply deformed rocks using porphyroblast inclusion trails. Tectonophysics 179, 353–369.
Hayward, N., 1992. Microstructural analysis of the classical spiral garnet porphyroblasts of south-east Vermont: evidence for non-rotation. Journal of Metamorphic Geology 10, 567–587.
Hebeda, E.H., Boelrijk, N.A.I.M., Priem, H.N.A., Verdurmen, E.A.T., Verschure, R.H., 1980. Excess radiogenic Ar and undisturbed Rb-Sr systems in basic intrusives subjected to Alpine metamorphism in southeastern Spain. Earth and Planetary Science Letters 47, 81–90.
Jabaloy, A., Galindo-Zaldivar, J., Conzález-Lodeiro, F., 1993. The Alpujárride-Nevado-Filábride extensional shear zone, Betic Cordillera, SE Spain. Journal of Structural Geology 15, 552–569.
Jabaloy-Sánchez, A. 1993. La estructura de la region occidental de la Sierra de los Filabres (Cordilleras Béticas). PhD Thesis, Universidad de Granada, 199 pp.
Johnson, S.E., 1990. Lack of porphyroblast rotation in the Otago Schists, South Island, New Zealand: implications for crenulation cleavage development, folding and deformation partitioning. Journal of Metamorphic Geology 8, 13–30.
Johnson, S.E., Dupee, M.E., Guidotti, C.V., 2006. Porphyroblast rotation during crenulation cleavage development: an example from the aureole of the Mooselookmeguntic pluton, Maine, USA. Journal of Metamorphic Geology 24, 55–73.
Jung, W.S., Ree, J.H., Park, Y., 1999. Non-rotation of garnet porphyroblasts and 3D inclusion trail data: an example from the Imjingang belt, South Korea. Tectonophysics 307, 381–395.
Konstantinovskaya, E.A., Malavieille, J., 2005. Accretionary orogens: Erosion and exhumation. Geotectonics 39, 69–86.
Langenberg, C.W., 1972. Polyphase Deformation in the Eastern Sierra de los Filabres, North of Lubrin, SE Spain. PhD Thesis. Gemeentelijke Universiteit Amsterdam, 81 pp.
Lonergan, L., White, N., 1997. Origin of the Betic- Rif mountain belt. Tectonics 16, 504–522.
Marín-Lechado, C., Galindo-Zaldívar, J., Rodríguez-Fernández, L.R., Serrano, I., Pedrera, A., 2005. Active faults, seismicity and stresses in an internal boundary of a tectonic arc (Campo de Dalías and Níjar, southeastern Betic Cordilleras, Spain). Tectonophysics 396, 81–96.
Martínez-Martínez, J.M., 1986a. Evolución tectonometamorpfica del complejo Nevado-Filabride en el sector de unión entre Sierra Nevada y Sierra de los Filabres (Cordilleras Beticas). PhD Thesis, Universidad de Granada, 194 pp.
Martínez-Martínez, J.M., 1986b. Fábricas y texturas miloníticas. Cinemática de las traslaciones en el complejo Nevado-Filabride (Cordilleras Béticas). Estudios Geológicos 42, 291–300.
Martinez-Martinez, J.M., 2006. Lateral interaction between metamorphic core complexes and less-extended, tilt-block domains: the Alpujarras strike–slip transfer fault zone (Betics, SE Spain). Journal of Structural Geology 28, 602–620.
Martínez-Martínez, J.M., Azañon, J.M., 1997. Mode of extensional tectonics in the southeastern Betics (SE Spain): Implications for the tectonic evolution of the peri-Alboran orogenic system. Tectonics 16, 205–225.
Martínez-Martínez, J.M., Soto, J.I., Balanyá, J.C., 2002. Orthogonal folding of extensional detachments: Structure and origin of the Sierra Nevada elongated dome (Betics, SE Spain). Tectonics 21, 1012, doi:10.1029/2001TC001283.
Michard, A., Chalouan, A., Feinberg, H., Goffé, B., Montigny, R., 2002. How does the Alpine belt end between Spain and Morocco? Bull. Soc. Géol. France 173, 3–15.
Monie, P., Torres-Roldán, R.L., Garcıcía-Casco, A., 1994. Cooling and exhumation of the Wertern Betic Cordilleras, 40Ar/39Ar thermochronological constraints on a collapsed terranes. Tectonophysics 238, 353–379.
Nijhuis, H.J., 1964. Plurifacial Alpine Metamorphism in the South-eastern Sierra de los Filabres, South of Lubrín, SE Spain. PhD Thesis. University of Amsterdam, Utrecht.
Orozco, M., Alonso-Chaves, F.M., Nieto, F., 1998. Development of large north-facing folds and their relation to crustal extension in the Alboran domain (Alpujarras region, Betic Cordilleras, Spain). Tectonophysics 298, 271–295.
Platt, J.P., Vissers, R.L.M., 1980. Extensional structures in anisotropic rocks. Journal of Structural Geology 2, 397–410.
Platt, J.P., Vissers, R.L.M., 1989. Extensional collapse of thickened continental lithosphere: A working hypothesis for the Alboran Sea and Gibraltar Arc. Geology 17, 540–543.
Platt, J.P., Van der Eeckhout, B., Janzen, E., Konert, G., Simon, O.J., Weijermars, R., 1983. The structure and tectonic evolution of the Aguilón foldnappe, Sierra Alhamilla, Betic Cordilleras, SE Spain. Journal of Structural Geology 5, 519–535.
Platt, J.P., Kelley, S.P., Carter, A., Orozco, M., 2005. Timing of tectonic events in the Alpujarride Complex, Betic Cordillera, southern Spain. Journal of the Geological Society 162, 451–462.
Platt, J.P., Anczkiewicz, R., Soto, J.I., Kelley, S.P., Thirlwall, M., 2006. Early Miocene continental subduction and rapid exhumation in the western Mediterranean. Geology 34, 981–984.
Platt, J.P., Behrmann, J.H., 1986. Structures and fabrics in a crustal sclae shear zone, Betic Cordillera, SE Spain. Journal of Structural Geology 8, 15–34.
Puga, E., 1990. The Betic Ophiolitic Association (southeastern Spain). Ofioliti 15, 97–117.
Puga, E., Diaz de Federico, A., Fontboté, J.M., 1974. Sobre la individualización y sistematización de las unidades profundas de la Zona Bética. Estudios Geológicos 30, 543–548.
Puga, E., Díaz de Federico, A., Nieto, J.M., 2002. Tectonostratigraphic subdivision and petrological characterisation of the deepest complexes of the Betic zone: a review. Geodinamica Acta 15, 23–43.
Puga, E., Fanning, M., Nieto, J.M., Díaz de Federico, A., 2004a. Recrystallization textures in zircon generated by ocean-floor and eclogite-facies metamorphism: a cathodoluminescence and U–Pb Shrimp study, with constraints from REE elements. The Canadian Mineralogist 43, 183–202.
Puga, E., Díaz de Federico, A., Nieto, J.M., Martín Algara, A., González Lodeiro, F., Estévez, A., Jabaloy, A., 2004b. Codilleras Beticas, Sucesiones Litológicas y petrología. In: Vera, J.A. (Ed.). Geología de España, Madrid, pp. 424–427.
Ramsay, J.G., 1962. The geometry and mechanism of formation of "similar" type folds. Journal of Geology 70, 309–327.
Rosenbaum, G., Lister, G.S., Duboz, C., 2002. Relative motions of Africa, Iberia and Europe during Alpine orogeny. Tectonophysics 359, 117–129.
Sayab, M., 2005. Microstructural evidence for N–S shortening in the Mount Isa Inlier (NW Queensland, Australia): the preservation of early W–E-trending foliations in porphyroblasts revealed by independent 3D measurement techniques. Journal of Structural Geology 27, 1445–1468.
Scherer, E.E., Cameron, K.L., Blichert-Toft, J., 2000. Lu–Hf garnet geochronology: Closure temperature relative to the Sm–Nd system and the effects of trace mineral inclusions. Geochimica et Cosmochimica Acta 64, 3413–3432.
Schettino, A., Turco, E., 2006. Plate kinematics of theWestern Mediterranean region during the Oligocene and Early Miocene. Geophysical Journal International 166, 1398–1423.

Soto, J.I., 1991. Estructura y evolución metamórfica del Complejo Nevado-Filábride en la terminación oriental de la Sierra de los Filabres (Cordilleras Béticas). PhD thesis, Universidad de Granada, 205 pp.

Stallard, A., Hickey, K., 2001. Shear zone vs folding origin for spiral inclusion trails in the Canton Schist. Journal of Structural Geology 23, 1845–1864.

Stípská, P., Schulmann, K., Kroner, A., 2004. Vertical extrusion and middle crustal spreading of omphacite granulite: a model of syn-convergent exhumation (Bohemian Massif, Czech Republic). Journal of Metamorphic Geology 22, 179–198.

Timms, N.E. Garnet porphyroblast timing and behaviour during fold evolution: implications from a 3D geometric analysis of a hand-sample scale fold in a schist. Journal of Metamorphic Geology 21, 853–873.

Vissers, R.L.M., 1981. A Structural Study of the Central Sierra de los Filabres (Betic Zone, SE SPain) with Emphasis on Deformational Processes and their Relation to the Alpine Metamorphism. PhD thesis. University of Amsterdam.

Vissers, R.L.M., Platt, J.P., Van der Wal, D., 1995. Late orogenic extension of the betic cordillera and the alboran domain—a lithospheric view. Tectonics 14, 786–803.

Yeh, M.W., 2007. Deformation sequence of Baltimore gneiss domes, USA, assessed from porphyroblast Foliation Intersection Axes. Journal of Structural Geology 29, 881–897.

Zeck, H.P., Whitehouse, M.J., 2002. Repeated age resetting in zircons from Hercynian-Alpine polymetamorphic schists (Betic–Rif tectonic belt, S. Spain)—a U-Th-Pb ion microprobe study. Chemical Geology 182, 275–292.